Hindawi
Geofluids
Volume 2021, Article ID 2071333, 9 pages
https://doi.org/10.1155/2021/2071333

Research Article

Geological Structure Exploration of Karst Collapse Column and Evaluation of Water Insulation Properties of the Mud Part

Shijian Yu[1], **Jiyang Liu**[1], **Peng Bai**[2], **Hongtao Xu**[2], **Runshan He**[2], **Yongshen Wang**[3] and **Dawei Yin**[1]

[1]*College of Safety and Environmental Engineering, Shandong University of Science and Technology, Qingdao, China 266590*
[2]*Shanxi Shiquan Coal Industry Co., Ltd., Changzhi, China 046020*
[3]*China Huadian Coal Industry Group Co., Ltd., Beijing, China 100035*

Correspondence should be addressed to Dawei Yin; 949251142@qq.com

Received 27 June 2021; Revised 7 September 2021; Accepted 8 September 2021; Published 26 September 2021

Academic Editor: Afshin Davarpanah

In this study, the X5 KCC in Shiquan Coal Mine was investigated by means of controlled source audio magnetotelluric exploration and borehole television. In this way, the subsection geological structure of the KCC was obtained. Next, the geological and electrical characteristics of each part were analyzed, and it is concluded that the development status of the mud part under coal seam floor is the key part to judging whether water inrush will occur during working face recovery under aquifer pressure. Furthermore, the mineral compositions of purplish-red mudstone and lime mudstone were obtained by performing an X-ray diffraction experiment on the KCC interstitial materials. On this basis, the water insulation properties of the mud part were qualitatively evaluated. Finally, the tensile strength of the mud part was obtained by the Brazilian splitting method, and the water insulation ability of the mud part at the periods when the tunneling roadway and the working face passed the KCC was calculated, respectively. The research results boast guiding significance for safe recovery of the working face passing KCCs under aquifer pressure.

1. Introduction

Karst collapse columns (KCCs) are a kind of special depression fault gradually formed in a long geological period under the condition of soluble rock strata and good groundwater dynamics [1]. The explanation for its cause includes the gypsum dissolution collapse theory [2], the gravitational collapse theory [3–5], the hydrothermal genesis theory [6], and the vacuum erosion collapse theory [7]. Generally, the formation of KCCs goes through four stages, namely, the early development stage, the intense development stage, the decline stage, and the death stage [8]. The formation process is controlled by factors such as geological environment, groundwater activity, geological structure, and stratigraphic lithologic combination. The material structure inside a KCC is complex and diverse, and the fabric characteristics of different parts differ obviously [9–11]. From the perspective of water inrush mechanism, a KCC can be divided into four parts, namely, the lower enrockment part, the middle mud part, the upper clast part, and the surrounding rock fracture part [12], and different parts correspond to varying fabric characteristics, water contents, and water conduction (insulation) properties. Water conduction of a KCC is related to the regional sedimentary environment, tectonic evolution, and karst water runoff conditions in the basement during its formation. After its formation, recompaction, cementation, weathering, and activation are the key factors [13–20]. The macroscopic subsection structure and water conduction (insulation) properties of a KCC are the geological basis to determine whether water inrush will occur when the KCC is exposed in the process of mining.

Seismic exploration, as the main method to explore KCCs from the perspective of geological structure, mainly solves the problem of KCC identification [21–25]. Electrical exploration, including the direct current method, the transient electromagnetic method, and the magnetotelluric

sounding method, which explores KCCs from the perspective of hydrogeology, mainly solves the problem of KCC water content [26–28]. These geophysical exploration methods interpret KCCs as a whole, without fully considering the characteristics of their subpart geological structure.

In this paper, mining under aquifer pressure when the tunneling roadway and the working face passed the X5 KCC in the 30107 fully mechanized working face of Shiquan Coal Mine was taken as the research background. Firstly, the subsection part geological structure of the X5 KCC was investigated by means of controlled source audio magnetotelluric (CSAMT) exploration and borehole television. Next, the tensile strength of rock in the mud part was obtained through the Brazilian splitting method. Furthermore, the water insulation capacities of the mud part when the tunneling roadway and the mining face passed the KCC were calculated, respectively. The research results provide geological basis for safe mining under aquifer pressure in the 30107 working face.

2. Development Characteristics of KCCs in Shiquan Coal Mine

2.1. Distribution Law of KCCs. Shiquan Coal Mine is located in Shiquan Village, Xiadian Town, 20.00 km west of Xiangyuan County, Changzhi City, Shanxi Province, China. Its maximum north-south length, maximum east-west width, and area are 6.00 km, 2.40 km, and 12.2195 km^2, respectively. The mining coal seam is No. 3 coal seam whose average thickness, mining elevation, and production scale are 6.0 m, +540~+70 m, and 1,200 kt/a, respectively.

Shiquan mine field is located in the east wing of Qinshui compound syncline and the west side of Jinhuo fold fault zone. Under such an influence, the strata belong to monoclinal structure (strike direction nearly south-north, dip direction west-northwest) with an inclination angle of 2°~25°. There are 48 faults and 23 KCCs in the mine field. In the north of the mine field, there are 7 secondary folds, and the strata are undulating. KCCs are usually densely distributed at positions where fractures, underground karst caves, and different tectonic systems are all highly developed. In Shiquan Coal Mine, KCCs are mostly distributed at the turning point of fold axis and near the fault, while they are rarely distributed far away from the fold axis or at positions where fractures are underdeveloped. The 23 identified KCCs are concentrated at or near the turning point of anticline axis.

2.2. Exposure Characteristics of the X5 KCC. The X5 KCC is exposed in the headgate of the 30107 face whose strike length and dip length are 1,530 m and 170 m, respectively. The mining coal seam is No. 3 coal seam whose average thickness is 6.0 m. The elevation of coal seam floor is +425~+530m, and that of Ordovician limestone water level is +636.87~+644.05 m. The 30107 working face is under aquifer pressure. According to the seismic exploration results, the plan shape of X5 KCC is like a dumbbell that is long in two sides and short in the middle, with a long-axis length of about 306 m and a short-axis length of about 75~100 m. The X5 KCC is exposed when the 30107 working face headgate is 530 m from the open-off cut. The exposure length is 98 m, including 78 m of whole rock. It extends into the 30107 working face for a maximum distance of 30 m. The position relationship is shown in Figure 1. The specific conditions of the X5 KCC are as follows.

The designed length of the 30107 headgate is 2,257.48 m. At 1,699 m in the 30107 headgate, the contact zone changes from the coal seam to the KCC. Specifically, the boundary on the lower side appears first, and the upper side lags for 4 m. In the broken zone, there are fine sandstone blocks with a size of over 1 m, small siltstone blocks and mudstone blocks, and the gaps among them are filled with argillaceous material; the accumulation body is dense and slightly wet. At 1,775 m in the 30107 headgate, the contact zone changes from the KCC to the coal seam. Specifically, the change occurs on the upper side first, and the lower side lags for 2 m. Figure 2 displays a longitudinal profile of the X5 KCC. Figure 3 shows a sketch of 30107 headgate passing through the X5 KCC and lithology photos of KCC exposed at different positions of roadway.

According to the classification of KCC structure with reference to literature [12] and the analysis on the actual disclosure situation, the KCC exposed in the 30107 headgate is located in the mudstone slurry water insulation part. Whether the 30107 working face can be safely mined under aquifer pressure depends on the thickness and water insulation ability of the mud part below the floor elevation of the 30107 face.

3. Analysis on the Geological Structure Exploration Results of X5

3.1. Results of Borehole Television Imaging Survey. In the hope of quantitatively determining the fracture development characteristics of the X5 KCC wall fracture part and the mud part, a borehole television imaging survey was conducted. The designed borehole passed through the KCC surrounding rock and the KCC body. The television image at the interface between the KCC surrounding rock and the KCC body is presented in Figure 4. The surrounding rock (siltstone) is an intact dark gray rock mass without developed fractures, indicating that the fractures in the KCC wall are underdeveloped in this part. The television image at the KCC body is illustrated in Figure 5. The KCC body has a pebbled structure, and the gravel is dark gray, grayish white, and brownish red; the gravel diameter ranges from 5 mm to 150 mm; the primary lithology is fine sandstone, and the cementing material is mainly dark gray mudstone, with local brownish red mudstone; the gravel content is about 50%, and no obvious fractures are found. The image suggests that the framework of the KCC fracture zone in this part is formed by the cementation of different-sized fine sandstone blocks, siltstone blocks, and mudstone blocks. The blocks are accumulated densely, resulting in underdeveloped fractures and low permeability. Thus, it is inferred that the KCC body can insulate water well.

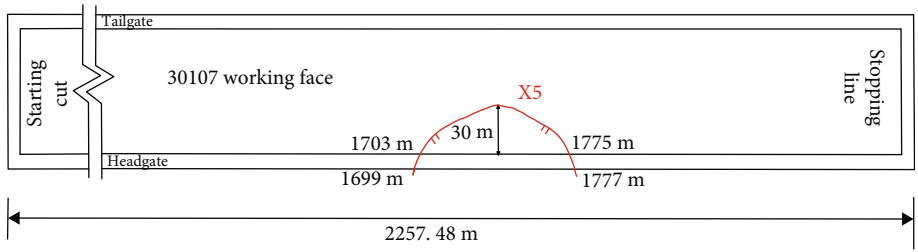

Figure 1: Plane position of the X5 FCC.

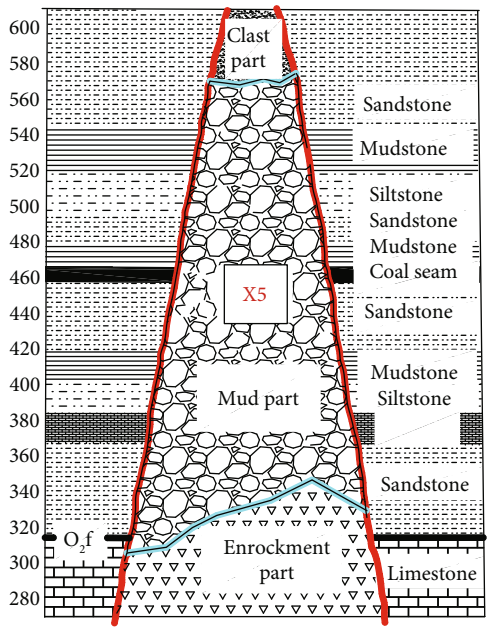

Figure 2: Longitudinal profile of the X5 KCC.

3.2. Results of CSAMT Exploration. To grasp the geological structure of the X5 KCC, the CSAMT geophysical exploration method was adopted. Taking the X5 KCC as the center, eleven 300 m long survey lines were laid along the vertical long axis, with the mesh degree being 10 × 50 m. The layout of survey lines is illustrated in Figure 6.

V8 System 2000.net, the eighth generation of geophysical data acquisition system of Phoenix Geophysical Co., Ltd., was adopted as the exploration equipment. In field observation, the bipolar source (AB = 1200 m) and the side E_x/H_y device were adopted; the measuring mode was scale TM; the measuring electrode distance Mn was 20 m; and the working frequency range is 0.52~5,120 Hz. A total of 38 frequency points were evenly distributed, avoiding 50 Hz, 60 Hz, and their multiple frequency points. The acquisition time for each frequency was longer than 40 s, and the number of single-frequency data stacking was not smaller than 40 times.

3.2.1. Structural Characteristics and Electrical Characteristics of Different Parts of the KCC. With respect to the macro structure, the KCC can be divided into three parts from bottom to top, namely, the enrockment part, the mud part, and the clast part. The electrical characteristics of the three parts differ significantly because of their varying components of filling materials at different heights, water contents, weathering degrees, and cementation degrees.

The enrockment part: located at the lower part of the KCC, the enrockment part was formed in the early stage of KCC formation. The collapse rock blocks were large in volume. Meanwhile, under the action of strong hydrodynamic pressure, fine rock debris and argillaceous material were taken away by the current, and the collapse deposits left were mostly large- and medium-sized rock blocks. This part usually contains some water, and its water content determines its electrical characteristics. When this part is of a large porosity and is filled with water, it shows a reduced resistivity in the transverse direction compared with the KCC surrounding rock strata; otherwise, it shows an increased resistivity.

The mud part: located in the middle of the KCC, the mud part was formed in the middle and late stage of KCC development. The solid materials in this part are the mixture of mud and collapse rock blocks from surrounding rock strata. Under the long-term action of in situ stress, the mixture gradually forms argillaceous cemented conglomerate. Generally speaking, this part of rock and soil mass is densely cemented with a high content of clay particles and low permeability. It neither contains water nor conducts water, belonging to a water insulation part of the KCC. Due to the existence of mudstone cement, it shows a decreased resistivity, compared with the KCC surrounding rock strata. The decrement depends on the content of mudstone cement. The higher the content of mudstone cement is, the more obviously the resistivity decreases.

The clastic part: located at the upper part of the KCC, the clast part is formed in the later stage of KCC development. In this part, rock blocks in the same stratum are arranged continuously, and the rock strata basically maintain continuity. Since the resistivity difference between the Carboniferous Permian upper strata is not large, the resistivity of this part is basically close to that of intact strata of the KCC surrounding rock, and the electrical anomaly characteristics are not obvious. In this part, the area affected by sandstone fracture aquifers and faults contains more water and is characterized by reduced resistivity.

3.2.2. Exploration Results. The resistivity parts of CSAMT sounding inversion on survey lines L3, L6, and L8 are displayed in Figure 7 which clearly reflects the macro geological structure of the X5 KCC, especially that of the water insulation mud part. As revealed by the analysis on the electrical

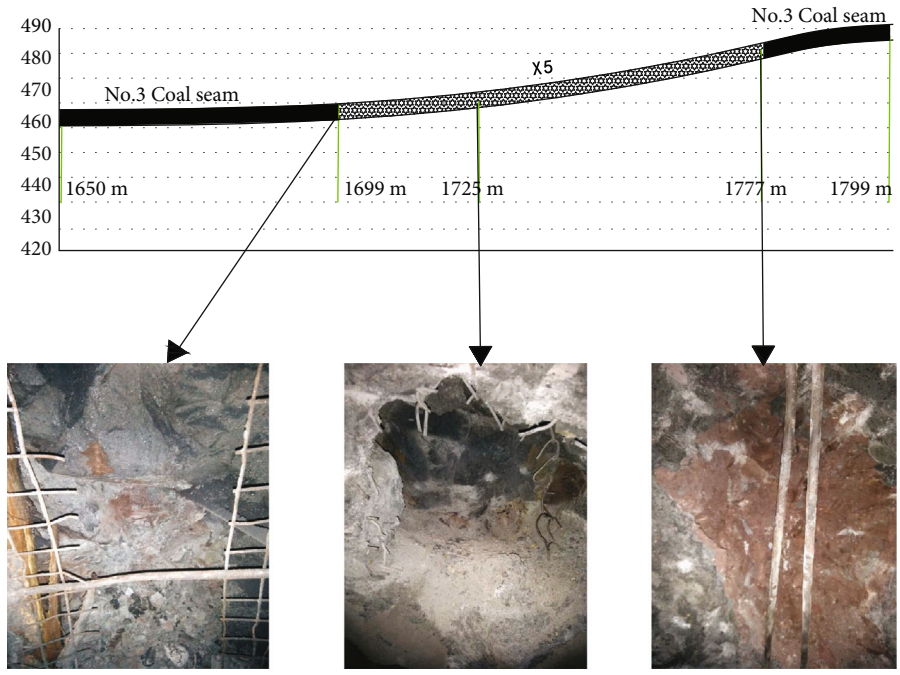

Figure 3: Sketch of 30107 headgate passing through X5 and lithology photos of KCC exposed at different positions of roadway.

characteristics of the three KCC parts, the mud part lies in the elevation ranges of +200~+600 m on the survey line L3, +380~+500 m on the L6 survey line, and +300~+440 m on the L8 survey line. The resistivity of rock mass in the clast part is slightly lower than that of surrounding rock mass, and its development depth is all above the elevation of No. 3 coal seam roof, but the development thickness tends to increase from southwest to northeast. Because of its high content (about 50%) of argillaceous cement, the resistivity of rock mass in the mud part is much lower than that of surrounding rock mass. The mud part below the elevation of No. 3 coal seam floor is thick on both sides and thin in the middle. To be specific, the maximum thicknesses in the southwest (survey line L3), in the middle (survey line L6), and in the northeast (survey line L8, corresponding to the 30107 headgate) are over 200 m, only 60 m, and over 100 m, respectively. The resistivity of rock mass in the enrockment part differs insignificantly from that of surrounding rock mass. It is inferred that the enrockment part has a relatively poor porosity and a low water content, and groundwater there has changed into fine fracture flow or pore seepage.

Based on the results of borehole television survey and CSAMT exploration, for No. 3 coal seam, the X5 KCC belongs to a muddy KCC with underdeveloped fractures on the wall. This type of KCC is filled with mud inside. In the mining process, the working face can advance safely as long as enough distance is kept from the water-containing enrockment part.

4. Evaluation of Water Insulation Properties of the Mud Part

4.1. X-Ray Diffractometry (XRD) Experiment on Interstitial Materials in the X5 KCC

4.1.1. Preparation of Experimental Samples. In the experiment, the purplish-red mudstone and lime mudstone from the interstitial materials in the X5 KCC were taken as the research objects, and the composition test and quantitative analysis were conducted on them with the aid of an XRD analyzer. First, the interstitial mudstone samples collected on site were broken into small particles, and then, the granular mudstone samples were ground into fine powder (generally 200~300 meshes) by using an agate mortar. The ground test samples were sealed in a sealed bag to avoid contact with air. During the experiment, the scanning range was set as 10°~90°, the scanning rate as 4°/min, and the scanning mode as fixed coupling.

4.1.2. Analysis on the Experimental Results. The XRD experiment was performed using the Rigaku D/Max 2500PC XRD instrument. The obtained .raw files were analyzed by Jade software. After interference removal and smoothing of the XRD spectra, the peak fitting conditions were set in accordance with the actual situation of the spectra. After fitting the peaks, qualitative analysis was conducted on the obtained peak parameters. The analysis results can reflect the components contained in the samples (Figure 8).

According to the XRD results, the main components of purplish-red mudstone are quartz, montmorillonite, albite, chlorite, calcite, kaolinite, and hematite and those of lime mudstone are quartz, montmorillonite, kaolinite, albite, and chlorite.

Table 1 shows the quantitative analysis results of XRD spectra. Purplish-red mudstone primarily contains quartz, montmorillonite, albite, chlorite, and calcite, as well as a little kaolinite and hematite. The proportion of quartz in lime mudstone is the highest, reaching 46.41%, while the proportions of montmorillonite, albite, chlorite, and kaolinite

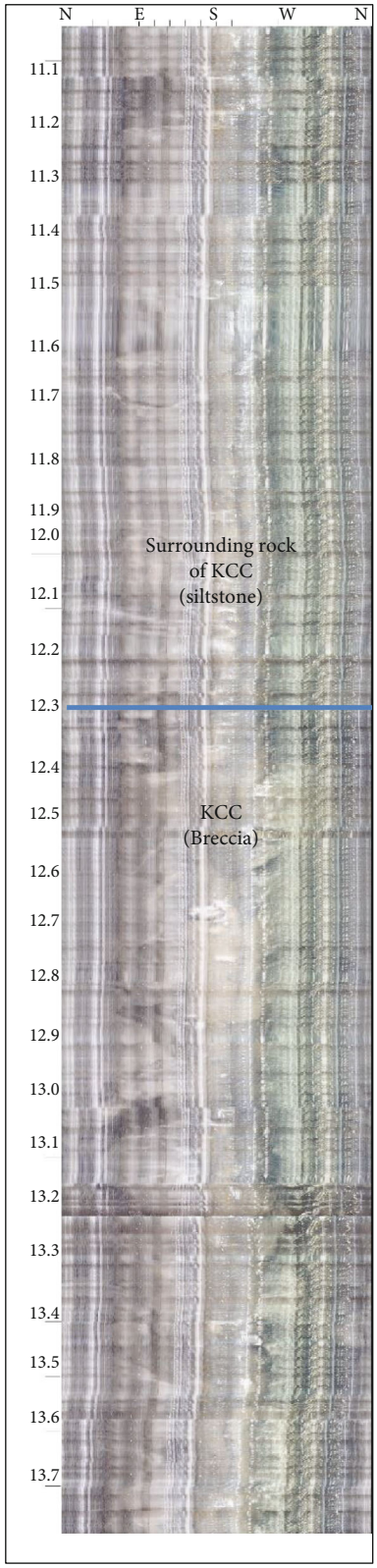

Figure 4: Television image of the interface between KCC surrounding rock and KCC body.

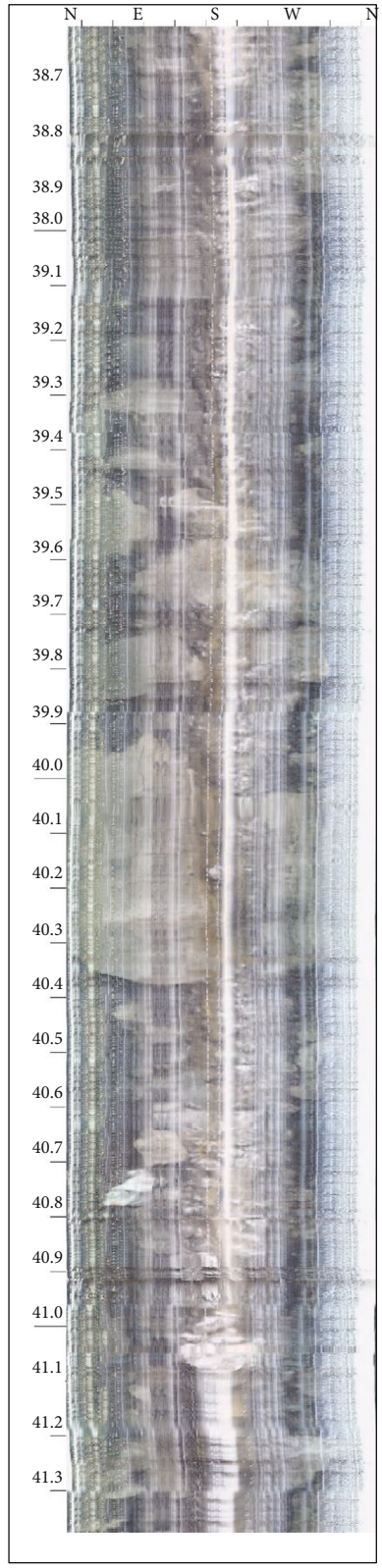

Figure 5: Television image of KCC body.

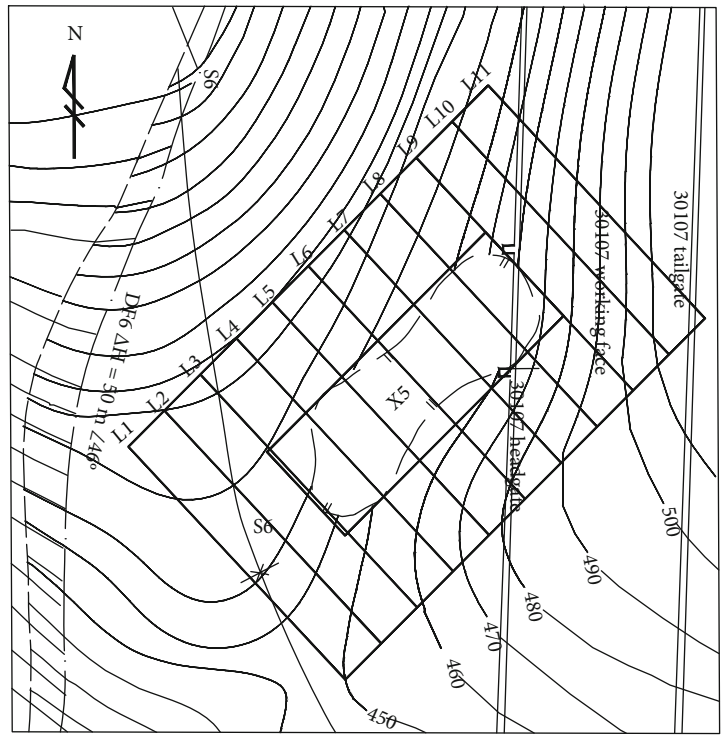

Figure 6: Layout of CSAMT survey lines in the X5 KCC.

resemble. The main components of the two kinds of stone are similar, but the kaolinite content is relatively high in lime mudstone and relatively low in purplish-red mudstone.

The kaolinite, montmorillonite, and chlorite in the interstitial minerals of the above samples belong to clay minerals which are characterized by plasticity, adhesiveness, and volume expansion when getting wet. The following phenomena are found during on-site exposure: the mixture of purplish-red mudstone, lime mudstone, and medium-fine grained sandstone occupies a relatively high proportion. No water seepage occurred throughout the entire disclosure process. The interface between the KCC and the coal seam is densely filled with argillaceous interstitial material, and no water erosion occurred, indicating that the mud part has a strong water insulation ability.

4.2. Uniaxial Tensile Test on the Water Insulation Layer of the Mud Part in the X5 KCC. The Shimazu AG-X250 electronic universal testing machine was used for uniaxial loading. In order to protect the Brazilian splitting test device, the loading adopted the displacement mode and was conducted at the rate of 0.01 mm/s. Table 2 shows the uniaxial tensile test results of X5 specimens.

The average tensile strength of the test specimens K_p = 0.78 MP, the standard variance $s = 0.145$, and the dispersion coefficient of the test results $\mu = s/S_t = 1.8\%$, which demonstrates that the average value of the test results is reliable and effective.

4.3. Evaluation of Water Insulation Ability of the Mud Part. According to *Rules for Coal Mine Water Prevention and Control*, the water insulation ability of tunneling roadway floor is calculated by Equation (1) [29]:

$$p = 2K_p \frac{t^2}{L^2} + \gamma t, \tag{1}$$

where p is the safe water pressure that the floor water insulation layer can bear, MPa; t is the thickness of the water insulation layer, m; L is the roadway width, and its value is 5 m; θ is the average weight of the floor water insulation layer, and its value is 0.022 MN/m^3; K_p is the average tensile strength of the floor water insulation layer, MPa.

The water insulation ability of the mining face is calculated by Equation (2) [29]:

$$P = T_s \times M, \tag{2}$$

where M is the thickness of the floor water insulation layer, M; P is the safe water pressure, MPa; T_s is the critical water inrush coefficient, MPa/m, and its value is 0.06 MPa/m in a tectonically deformed part.

According to the CSAMT exploration results, the water insulation mud part below the 30107 headgate floor is 100 m thick. As can be calculated by Equation (1), the water insulation layer below the X5 KCC of the 30107 face tunnelling roadway floor can bear a maximum aquifer pressure of 626.2 MPa. In addition, according to the elevation (460 m) of No. 3 coal seam floor during the exposure of the X5 KCC in the headgate and the current Ordovician limestone water level (636.87 m) in Shiquan mine field, the water pressure at the bottom of the mud part is calculated to be 2.71 MPa, and the thickness of the water insulation layer is calculated

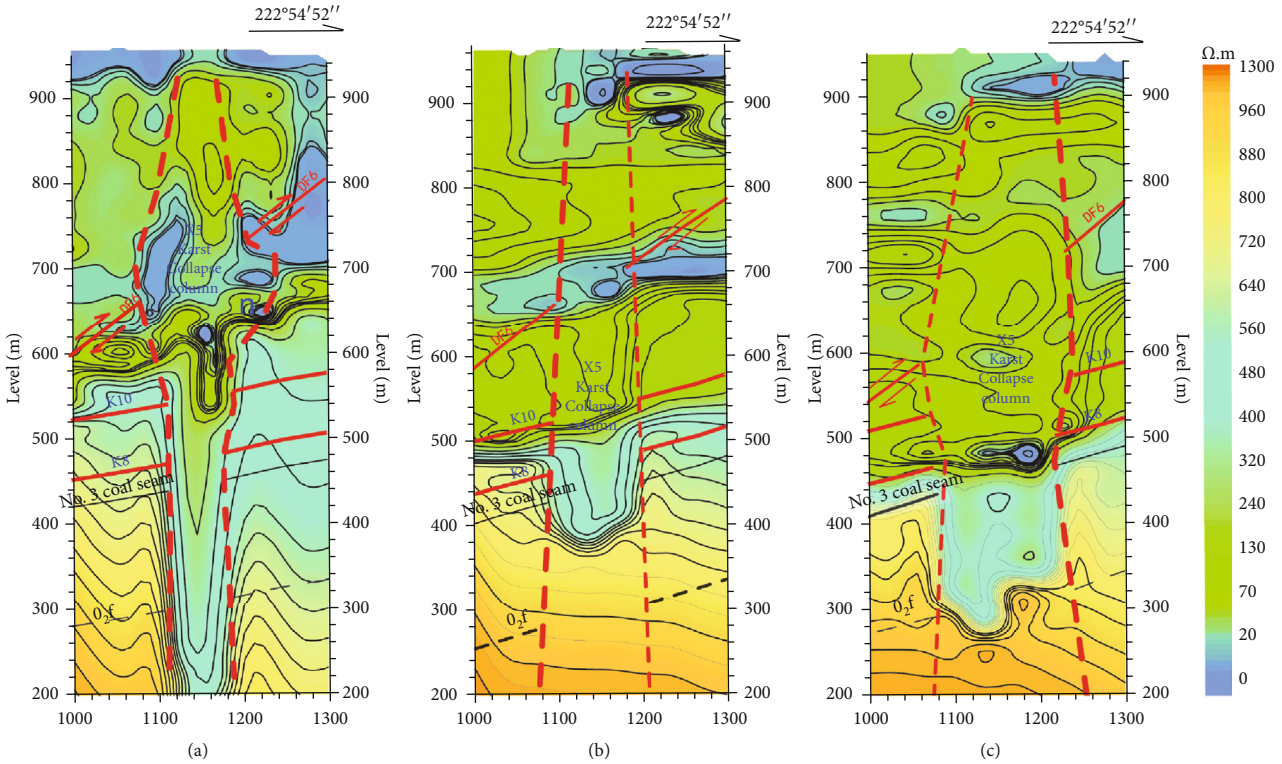

Figure 7: Resistivity part of CSAMT sounding inversion.

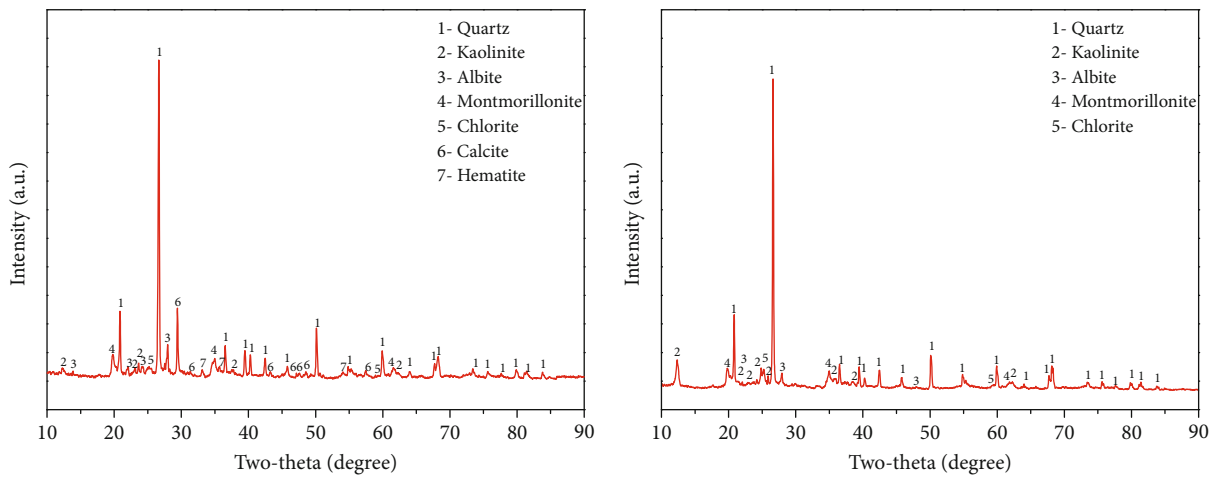

(a) XRD spectrum of purplish-red mudstone

(b) XRD spectrum of lime mudstone

Figure 8: XRD spectra.

to be 45.1 m by Equation (2). Considering the above data, it is judged that the 30107 face can pass the X5 KCC safely without encountering inrush of Ordovician limestone confined water.

5. Discussions

5.1. KCC Occurrence State. Due to the differences in regional geological and hydrogeological conditions, sedimentary environment, and stratigraphic lithologic assemblage, the geological structures of KCCs exhibit significant regional and individual differences. The existence of a mud part is a necessary condition to ensure no water inrush when a working face passes a KCC under aquifer pressure, but it is not a sufficient condition, because whether the working face can advance safely also depends on the thickness and water insulation ability of the mud part below the working face floor. The exploration results of the X5 KCC suggest that the mud part is thick on both sides and thin in the middle. According to the exposure conditions, the KCCs passed

Table 1: Mineral composition of interstitial materials.

Interstitial material	Composition (%)							
	Quartz	Montmorillonite	Kaolinite	Sodium feldspar	Chlorite	Calcite	Hematite	Other
Purplish-red mudstone	41.15	18.67	3.6	15.36	10.41	6.95	1.21	2.65
Grey mudstone	46.41	16.79	13.56	10.72	8.27	—	—	3.25

Table 2: Uniaxial tensile test results of X5 specimens.

Specimen No.	Diameter (mm)	Thickness (mm)	Breaking load (KN)	Tensile strength (MPa)
1	50.16	26.76	1.586	0.752
2	50.02	26.78	1.439	0.684
3	50.22	24.12	1.798	0.945
4	50.58	24.40	1.409	0.727
5	49.96	25.10	1.607	0.816

during the mining of No. 3 coal seam all lie in the mud part, which provides necessary geological conditions for safe recovery of the working face passing KCCs under aquifer pressure.

5.2. Geological Conditions and Genesis of KCC. The KCCs in Shiquan mine field own the geological conditions for the formation of a water insulation mud part. The material basis of a mud part is the formation of dissolvable and decomposable strata, such as mudstone, shale, and argillaceous limestone. After these strata collapse, they can decompose rapidly under the dynamic action of solid-liquid-gas three phases and combine with water to form mud. The formed mud, together with the collapsed surrounding rock strata, compose the solid material of the mud part. The Permian strata in Shiquan mine field (Shanxi Formation and Lower Shihezi Formation in the lower part, Upper Shihezi Formation, and Shiqianfeng Formation in the upper part) are deltaic continental deposits (266~422 m thick) composed of conglomerate, sandstone, siltstone, mudstone, and coal seam. Specifically, Shanxi Formation is mainly composed of black mudstone, dark gray sandy mudstone, siltstone, and gray and gray-white sandstone. Lower Shihezi Formation is composed of gray sandstone interspersed with gray and gray-black mudstone, sandy mudstone, and siltstone; the top is a stable layer of gray green, yellow green, and purple variegated mudstone that contains iron and manganese nodules, commonly known as peach blossom mudstone; the cemented material observed during the exposure of the X5 KCC in the 30107 headgate is just the peach blossom mudstone. Upper Shihezi Formation, which belongs to continental fluvial and lacustrine deposits, is composed of variegated sand and mudstone. Sedimentary characteristics of the Permian strata determine that there is sufficient mudstone slurry to fill the gaps between sandstone blocks and limestone blocks during the formation of KCCs. Under the long-term action of gravity, mudstone slurry material begins to consolidate, solidify, and rheology, gradually forming conglomerate similar to mudstone cement. This is the geological reason why the mud part of the X5 KCC below the elevation of No. 3 coal seam floor is 60~100 m thick. The fabric characteristics (about 50% of argillaceous cement and about 50% of breccia) and the electrical characteristics of the mud part of the KCC developed in Shiquan mine field provide the physical conditions for the accurate classification of the mud part by the electrical exploration method.

6. Conclusions

(1) The KCC in Shiquan mine field has clear subparts in geological structure, and the thickness and water insulation ability of the mud part in the No. 3 coal seam floor are the geological basis for determining whether water inrush will occur when the KCC is exposed in the process of mining

(2) CSAMT exploration and borehole television are effective technical means to divide the geological subparts of the KCC

(3) The interstitial minerals in the mud part are rich in clay minerals such as kaolinite, montmorillonite, and chlorite which are characterized by plasticity, adhesiveness, and volume expansion when getting wet. They are the material basis for the strong water insulation ability of the mud part

(4) Under the sedimentary environment of continental river and lake, dissolvable and decomposable strata, such as mudstone, shale, and argillaceous limestone, are formed in Shiquan mine field, which is the geological reason for the formation of the water insulation mud part. The fabric characteristics of about 50% argillaceous cement and about 50% breccia guarantee the strong water insulation ability of the mud part

Data Availability

The data used to support the findings of this study are included in the article.

Conflicts of Interest

The authors declare that they have no conflicts of interest.

Acknowledgments

This work was supported by the National Science Foundation of China (51904167), the Taishan Scholars Project, the Taishan Scholar Talent Team Support Plan for Advantaged

and Unique Discipline Areas, and the SDUST Research Fund (2018TDJH102).

References

[1] S. X. Yin, H. Q. Lian, and D. M. Liu, "70 years of investigation on karst collapse column in North China Coalfield: cause of origin, mechanism and prevention," *Coal Science and Technology*, vol. 47, no. 11, pp. 1–29, 2019.

[2] X. P. Qian, "Formation of gypsum karst collapse column and its hydro - geological significance," *Carsologica Sinica*, vol. 7, no. 4, pp. 70–74, 1988.

[3] R. Wang, "Discussion on the causes and prevention of ground collapse in karst mining area," *Hydrogeology & Engineering Geology*, vol. 26, no. 1, pp. 37–41, 1982.

[4] W. M. Yang and Z. A. Zhou, "Analysis of rock mass structure of karst collapse column," *Journal of Huainan Mining Institute*, vol. 17, no. 2, pp. 1–7, 1997.

[5] B. L. Hu and X. M. Song, "Deep karst cave and collapse column formation mechanism in Huaibei coalfield," *Coal Geology of China*, vol. 9, no. 2, pp. 47–49, 1997.

[6] S. P. Chen, "Discussion on the cause of karst collapse column in Fengfeng area of Hebei Province," *Carsologica Sinica*, vol. 12, no. 3, pp. 52–63, 1993.

[7] W. G. Xu and G. R. Zhao, "The implication of suction action for ground subsidence in karst mining areas," *Geological Review*, vol. 27, no. 2, pp. 86–95, 1981.

[8] Y. J. Li and S. P. Peng, "Classifications and characteristics of karst collapse columns in North China coalfields," *COAL-GEOLOGY& EXPLORATION*, vol. 34, no. 4, pp. 53–57, 2006.

[9] J. G. Zhao, M. T. Guo, and W. S. Li, "Morphological and fabric characteristics of karst collapse pillars in Xishan coalfield," *Journal of China Coal Society*, vol. 45, no. 7, pp. 2389–2398, 2020.

[10] S. X. Yin, Q. Wu, and S. X. Wang, "Studies on characters and forming mechanism of karstic collapse columns at mine area of North China," *Chinese Journal of Rock Mechanics and Engineering*, vol. 23, no. 1, pp. 120–123, 2004.

[11] Z. Q. She, "Characteristics and prediction methods of ancient karst columnar collapse," *Coal Geology & Exploration*, vol. 18, no. 2, pp. 42–45, 1990.

[12] L. Niu, Q. Wu, and B. Li, "Classification of karst collapse columns in North China coalfields based on the generalized model of inside structure of the columns," *Coal Geology & Exploration*, vol. 43, no. 3, pp. 56–60, 2015.

[13] S. X. Yin, Q. Wu, and S. X. Wang, "Water-bearing characteristics and hydro-geological models of karstic collapse pillars in north China," *Journal of Rock Mechanics and Geotechnical Engineering*, vol. 24, no. 1, pp. 77–82, 2005.

[14] W. J. Yu and K. Li, "Deformation mechanism and control technology of surrounding rock in the deep-buried large-span chamber," *Geofluids*, vol. 2020, 22 pages, 2020.

[15] W. J. Yu, G. S. Wu, and B. Pan, "Experimental investigation of the mechanical properties of sandstone–coal–bolt specimens with different angles under conventional triaxial compression," *International Journal of Geomechanics*, vol. 21, no. 6, p. 04021067, 2021.

[16] W. J. Yu, K. Li, and Z. Liu, "Mechanical characteristics and deformation control of surrounding rock in weakly cemented siltstone," *Environmental Earth Sciences*, vol. 80, no. 9, 2021.

[17] D. Ma, J. X. Zhang, and Y. L. Huang, "Reutilization of gangue wastes in underground backfilling mining: overburden aquifer protection," *Chemosphere*, vol. 264, p. 128400, 2021.

[18] H. Wu, D. Ma, and A. J. S. Spearing, "Fracture phenomena and mechanisms of brittle rock with different numbers of openings under uniaxial loading," *Geomechanics and Engineering*, vol. 25, no. 6, pp. 481–493, 2021.

[19] D. Ma, B. K. Sai, and Z. H. Li, "Effect of wetting-drying cycle on hydraulic and mechanical properties of cemented paste backfill of the recycled solid wastes," *Chemosphere*, vol. 282, p. 131163, 2021.

[20] D. Ma, J. J. Wang, and X. Cai, "Effects of height/diameter ratio on failure and damage properties of granite under coupled bending and splitting deformation," *Engineering Fracture Mechanics*, vol. 220, p. 106640, 2019.

[21] S. H. Wu, G. X. Zhou, and S. X. Yang, "Analys is for the seismic response characteristics of collapse column," *Coal Geology & Exploration*, vol. 32, 2004.

[22] J. H. Ning and G. Z. Zhang, "Seismic identification technique and its application of collapse column," *Coal Geology & Exploration*, vol. 33, no. 3, pp. 64–67, 2005.

[23] J. P. Zuo, S. P. Peng, and Y. J. Li, "Investigation of karst collapse based on 3-D seismic technique and DDA method at Xieqiao coal mine, China," *International Journal of Coal Geology*, vol. 78, no. 4, pp. 276–287, 2009.

[24] Q. F. Yin, D. M. Pan, J. C. Yu, and S. D. Liu, "Research on seismic identification technique of coal mine collapse column," *Progress in Geophysics*, vol. 27, no. 5, pp. 2168–2174, 2012.

[25] B. W. Han, X. B. Liu, and Q. Li, "Coalfield subsided column and gob area identification through 3D seismic interpretation," *Coal Geology of China*, vol. 27, no. 9, pp. 67–70, 2015.

[26] J. L. Cheng, F. Li, and S. P. Peng, "Research progress and development direction on advanced detection in mine roadway working face using geophysical methods," *Journal of China Coal Society*, vol. 39, no. 8, pp. 1742–1750, 2014.

[27] G. Q. Xue and J. C. Yu, "New development of TEM research and application in coal mine exploration," *Progress in Geophysics*, vol. 32, no. 1, pp. 319–326, 2017.

[28] J. S. An, Q. X. Sun, and H. Qiu, "Experimental study on underground collapse column by integrated detection technology," *Coal Science and Technology*, vol. 43, no. 10, pp. 144–147, 2015.

[29] State Administration of Coal Mine Safty, *Rules for Coal Mine Water Prevention and Control*, Beijing, China Coal Industry Publishing House, 2018.